The American Journal of Pathology, Vol. 170, No. 3, March 2007

DOI: 10.2353/ajpath.2007.060428

Cell Injury, Repair, Aging and Apoptosis

Protein Characterization of Na^+-Independent System L Amino Acid Transporter 3 in Mice

A Potential Role in Supply of Branched-Chain Amino Acids under Nutrient Starvation

Daisuke Fukuhara,* Yoshikatsu Kanai,† Arthit Chairoungdua,† Ellappan Babu,† Fumio Bessho,* Toshio Kawano,* Yoshihiro Akimoto,‡ Hitoshi Endou,† and Kunimasa Yan*

From the Departments of Pediatrics, Toxicology and Pharmacology,† and Anatomy,‡ Kyorin University School of Medicine, Tokyo, Japan*

We recently cloned the human Na^+-independent system L neutral amino acid transporter LAT3. The aim of the present study was to characterize the molecular nature of mouse LAT3 at the protein level. Isolated mouse LAT3 showed 83% identity to human LAT3. *Xenopus* oocytes injected with mouse LAT3 cRNA showed the same functional property as human LAT3. Reverse transcriptase-polymerase chain reaction revealed apparent transcripts of mouse LAT3 in the liver, skeletal muscle, and pancreas, an expression pattern identical to that found in humans. Antibody generated against mouse LAT3 detected both ~58-kd and 48-kd bands in the sample from liver and only a 48-kd band in skeletal muscle and pancreas. Immunohistochemical study showed its clear localization in the plasma membrane of liver and skeletal muscle, whereas it was only detectable in the endoplasmic reticulum and in crystalline inclusions in pancreatic acinar cells. Starvation induced up-regulation of mouse LAT3 protein and mRNA in both liver and skeletal muscle but not in pancreas. These results suggest that LAT3 may indeed function as an amino acid transporter, transporting branched-chain amino acids from liver and skeletal muscle to the bloodstream and thereby participating in the regulatory system of interorgan amino acid nutrition. ***(Am J Pathol 2007, 170:888–898; DOI: 10.2353/ajpath.2007.060428)***

Amino acid transport across the plasma membrane regulates the flow of these nutrients into cells or from cells and thus participates in interorgan amino acid nutrition. The transfer of amino acids across the hydrophobic domain of the plasma membrane is mediated by specific transporter proteins that recognize, bind, and transfer amino acids from the extracellular space into cells or vice versa.[1,2] The transport of neutral amino acids through the plasma membrane is mediated via Na^+-dependent and Na^+-independent transport systems[1,2] in which Na^+-independent system L is one of the major routes to provide cells with branched-chain amino acids (BCAAs) and aromatic amino acids. By means of expression cloning, we identified the first isoform of Na^+-independent system L amino acid transporter LAT1 (L-type amino acid transporter 1) from C6 rat glioma cells.[3] LAT1 is a member of the SLC (solute carrier) 7 family and mediates a Na^+-independent amino acid exchange, preferring large neutral amino acids such as leucine, isoleucine, valine, phenylalanine, tyrosine, tryptophan, methionine, and histidine as its substrates. Following the identification of LAT1, a second system L transporter, named LAT2, was identified by various groups including ours.[4–6] LAT2 is more ubiquitously expressed than LAT1 and transports not only large neutral amino acids but also small ones. As a common molecular feature of LAT1 and LAT2, they form the same heteromeric complexes via a disulfide bond with a single membrane-spanning protein, the heavy chain of 4F2 antigen, which is essential for the functional

Supported by The Ministry of Education, Culture, Sport, Science and Technology of Japan, KAKENHI (C18590901); a grant from the Promotion and Mutual Aid Corporation for Private Schools of Japan; a grant from Novartis Pharma K.K.; and a grant from Morinaga.

Accepted for publication November 17, 2006.

Address reprint requests to Kunimasa Yan, Department of Pediatrics, Kyorin University School of Medicine, Mitaka, Tokyo 181-8611, Japan. E-mail: kuniyan@kyorin-u.ac.jp.

expression of both LAT1 and LAT2 in the plasma membrane.[3–7]

Even after the identification of these heteromeric amino acid transporters, some of the previously reported properties of system L remained to be explained in light of the properties of LAT1 and LAT2. Recently, we isolated a cDNA encoding a novel Na^+-independent neutral amino acid transporter from human hepatocarcinoma cells, FLC4, by expression cloning.[8] This gene product, designated LAT3, is predicted to be a 12-transmembrane domain protein containing a relatively long extracellular loop with putative N-linked glycosylation sites between transmembrane domains 1 and 2. A long intracellular loop, predicted to exist between transmembrane domains 6 and 7, contains putative protein kinase C-dependent phosphorylation sites and a tyrosine phosphorylation site. Northern blot analysis using human multiple tissue Northern blots indicated that its message is highly expressed in the liver, pancreas, and skeletal muscle. However, its molecular nature and role in the regulatory system of the interorgan amino acid nutrition remains largely to be elucidated. In the present study, to characterize LAT3, we first isolated LAT3 cDNA from mouse and then determined the protein expression and distribution of the transporter in the liver, pancreas, and skeletal muscle. Moreover, we also obtained data indicating that LAT3 may participate in the supply of BCAAs from the liver and skeletal muscle to other organs under the nutrient-starved condition.

Materials and Methods

Animals

Eight-week-old male ICR mice (26 to 28 g; Saitama, Japan) were anesthetized by intraperitoneal injection with pentobarbital. For the histological experiments, tissues were embedded in Tissue-Tek OCT compound (Sakura Fine Technical Co., Tokyo, Japan). Tissues were also rapidly frozen and stored in liquid nitrogen for the isolation of total RNA and the membrane fraction. For the starvation studies, eight mice were deprived of food for 24 hours[9–10] but were free to drink water. Another eight mice with access to both food and water were examined as the control.

cDNA for Mouse LAT3

The cDNA for a mouse expressed sequence tag (GenBank/European Bioinformatics Institute/DNA Databank of Japan accession number BG865268) showing nucleotide sequence similarity to human LAT3[8] was obtained from Integrated and Molecular Analysis of Genomes and their Expression (IMAGE cDNA clone number 4910149). The cDNA insert was subcloned into the mammalian expression vector pcDNA 3.1(+) at *Not*I and *Hind*III restriction enzyme cleavage sites. The cDNA was sequenced in both directions by dye terminator cycle sequencing (Applied Biosystems, Foster City, CA).

Functional Characterization of Mouse LAT3

cRNA for mouse LAT3 was obtained by *in vitro* transcription using SP6 RNA polymerase from the mouse LAT3 cDNA in plasmid pSPORT6 linearized with *Not*I. Three days after *Xenopus* oocytes were injected with 25 ng of the synthesized cRNA, the uptake of ^{14}C-labeled amino acids was measured in the regular uptake solution (100 μmol/L NaCl, 2 mmol/L KCl, 1 mmol/L $CaCl_2$, 1 mmol/L $MgCl_2$, 10 mmol/L HEPES, and 5 mmol/L Tris, pH 7.4) or Na^+-free uptake solution in which NaCl in the regular uptake solution was replaced by 100 μmol/L choline chloride.[11,12] For Cl^--free uptake solution, Cl^- in the regular uptake solution was replaced by gluconate anion. The uptake levels were measured for 30 minutes, and the values were expressed as picomoles/oocyte/minute.

DNA Transfection

The human embryonic kidney cell line (HEK 293) was grown in Dulbecco's modified Eagle's medium (Life Technologies, Gaithersburg, MD) supplemented with 10% fetal calf serum and 100 U/ml penicillin/streptomycin in a 37°C incubator with 5% CO_2. For the transient transfection with the mouse LAT3 construct, HEK 293 cells were plated onto 60-mm dishes and transfected with 2 μg of plasmid DNA containing or lacking the human LAT3 construct by using FuGene6 (Roche Diagnostics, Basel, Switzerland) according to the manufacturer's protocol.

RNA Extraction and Reverse Transcriptase-Polymerase Chain Reaction (RT-PCR)

Total RNA was extracted from HEK 293 cells transfected with the mouse LAT3 construct and from mouse tissues using Isogen (Wako Life Science Reagents, Osaka, Japan) according to the manufacturer's instructions. RT-PCR analysis was performed by using the sense primer 5′-GGCACCACCATCTCCAAGTC-3′ (nucleotides 322 to 341) and the antisense primer 5′-TAGGCCAGGTTCGTCAGCAC-3′ (nucleotides 883 to 902) for mouse LAT1; the sense primer 5′-GGCGTCACCATCCCTAAGTC-3′ (nucleotides 286 to 305) and the antisense primer 5′-CCATGACCCCGAGGAGTTTC-3′ (nucleotides 921 to 940) for mouse LAT2; the sense primer 5′-GTGACTGGTGGCAAGGAACG-3′ (nucleotides 997 to 1016) and the antisense primer 5′-AGTAGGAGGCCCAGGTTCAC-3′ (nucleotides 1549 to 1568) for mouse LAT3; and sense primer 5′-GACAACGGCTCCGGCATGTGCA-3′ (nucleotides 31 to 52) and antisense primer 5′-ATGACCTGGCCGTCAGGCAGCT-3′ (nucleotides 722 to 743) for mouse β-actin. One microgram of total RNA was amplified under the following conditions: 30 amplification cycles of 94°C for 1 minute, 63°C for 1 minute, and 72°C for 1 minute. Amplification was completed with prolonged synthesis at 72°C for 10 minutes. PCR products were visualized by ethidium bromide staining following electrophoresis on a 4% NuSieve 3:1 agarose gel (BioWhittaker Molecular Applications, Rockland, ME).

Antibodies

Anti-mouse LAT3 polyclonal antibody was generated against a synthetic peptide corresponding to TGGKERETNEQRQ (amino acids 336 to 348 of the intracellular domain: referred to as peptide II) of the LAT3 amino acid sequence. To verify further the specificity of this antibody, we also synthesized two other peptides, VTGGKERETNEQRQK (amino acids 335 to 349, referred to as peptide III) and TGGKERETN (amino acids 336 to 344, referred to as peptide I), and preincubated them with the anti-mouse LAT3 antibody for use in the Western blot analysis described below. A rabbit was immunized with 0.5 mg of peptide II conjugated to the carrier protein keyhole limpet hemocyanin and boosted three times with 0.5 mg of the immunogen each time. The rabbit was sacrificed and bled 10 days after the last immunization. The antiserum was affinity-purified with the corresponding peptide linked to CNBr-activated Sepharose 4B column (Pharmacia, Piscataway, NJ). The following antibodies were purchased from the suppliers as indicated: horseradish peroxidase (HRP)-labeled goat anti-rabbit immunoglobulins (Dako, Carpinteria, CA), Alexa Fluor 488-conjugated goat anti-rabbit IgG (Molecular Probes, Eugene, OR), and colloidal gold (12 nm)-labeled donkey anti-rabbit IgG (Jackson Immunoresearch Laboratories, West Grove, PA).

Western Blot Analysis

Western blot analysis was performed as previously described.[13,14] Briefly, membrane fractions from mouse tissues were isolated by using a subcellular proteome extraction kit (ProteoExtract; Calbiochem, Darmstadt, Germany) according to the manufacturer's instructions. Samples were mixed with an equal volume of sample buffer [125 mmol/L Tris-HCl, 1% sodium dodecyl sulfate (SDS), 5% sucrose, and 0.1% bromphenol blue], and the proteins were separated by 10% SDS-polyacrylamide gel electrophoresis and transferred to polyvinylidene difluoride membranes. After a blocking procedure, the membranes were reacted with anti-mouse LAT3 antibody (0.5 μg/ml) or anti-LAT3 antibody preabsorbed by each synthesized peptide including the immunogen peptide described above. Reaction sites were visualized by using the combination of horseradish peroxidase (HRP)-labeled goat anti-rabbit antibody (1:2000) and a chemiluminescence kit (Life Science Products, Boston, MA) according to the manufacturer's instructions.

Immunohistochemistry

Frozen sections from the mouse tissues were fixed in 4% paraformaldehyde-0.1 mol/L phosphate-buffered saline (PBS) for 10 minutes at room temperature. After having been washed with PBS, the slides were incubated with blocking buffer (3% bovine serum albumin, 5% goat serum, and 0.05% Tween 20 in PBS) and then reacted with anti-mouse LAT3 antibody (5 μg/ml) or anti-mouse LAT3 antibody preabsorbed with the immunogen peptide (5 μg/ml) overnight at 4°C. After another wash with PBS, the slides were incubated with HRP-labeled goat anti-rabbit antibody (1:200) at room temperature, and then the slides were developed by immersion in 1.4 mmol/L 3,3′-diaminobenzidine tetrahydrochloride (Sigma Chemical Co., St. Louis, MO) in PBS. Hematoxylin was used as a counterstain.

Immunofluorescence and Confocal Microscopy

Frozen sections of the tissue samples from fed mice and starved ones were fixed as described above. After having been washed with PBS, the slides were incubated with blocking buffer for 60 minutes and then reacted with anti-LAT3 antibody (5 μg/ml) overnight at 4°C. After another wash with PBS, the slides were incubated with Alexa Fluor 488-conjugated goat anti-rabbit IgG (5 μg/ml) for 60 minutes at room temperature. After a final PBS wash, the slides were mounted in 1 mg/ml *p*-phenylenediamine in PBS/glycerol (1:1) and examined under a confocal laser scanning microscope equipped with a krypton/argon laser (model MRC1024; Bio-Rad, Hercules, CA).[14,15]

Electron Microscopy

Tissue samples were fixed in phosphate-buffered 2.5% glutaraldehyde (pH 7.4), postosmicated, and dehydrated by passage through graded alcohols as previously described.[16] Briefly, after immersion in propylene oxide, the specimens were embedded in Epon 812. Ultrathin sections were cut perpendicular to the epithelium, doubly stained with uranyl acetate and lead citrate, and examined with a transmission electron microscope (model TEM-1010C; JEOL, Tokyo, Japan).

Immunogold Labeling for Electron Microscopy

Immunogold labeling was performed as described previously.[17,18] The pancreas was fixed in 4% paraformaldehyde-PBS for 2 hours at 4°C. After the specimens were washed with PBS, they were dehydrated through a series of graded ethanols and then embedded in LR White resin (London Resin, Basingstoke, UK). Ultrathin sections were cut and mounted on nickel grids. The sections were incubated with 5% normal donkey serum in PBS for 1 hour and subsequently with anti-mouse LAT3 antibody (5 μg/ml) at 4°C for 24 hours. As an immunocytochemical control, some samples were incubated with nonimmunized rabbit IgG. Following a PBS wash, the samples were incubated with 12-nm colloidal gold-conjugated donkey anti-rabbit IgG antibody for 2 hours at room temperature. Thereafter they were washed with PBS and then fixed in 2% glutaraldehyde. After having been rinsed with deionized water, the ultrathin sections were stained with uranyl acetate and observed under a transmission electron microscope (model JEM-1010; JEOL).

```
Mouse LAT3      MAPTLKQAYRRRWWMACTAVVENLFFSAVLLGWASLLIMLKKEGFYSSLCPAENRTNTTQ
Human LAT3      MAPTLQQAYRRRWWMACTAVLENLFFSAVLLGWGSLLIILKNEGFYSSTCPAESSTNTTQ

Mouse LAT3      DEQHQWTSCDQQEKMLNLGFTIGSFLLSATTLPLGILMDRFGPRPLRLVGSACFAASCTL
Human LAT3      DEQRRWPGCDQQDEMLNLGFTIGSFVLSATTLPLGILMDRFGPRPVRLVGSACFTASCTL

Mouse LAT3      MALASRDTEVLSPLIFLALSLNGFAGICLTFTSLTLPNMFGNLRSTFMALMIGSYASSAI
Human LAT3      MALASRDVEALSPLIFLALSLNGFGGICLTFTSLTLPNMFGNLRSTLMALMIGSYASSAI

Mouse LAT3      TFPGIKLIYDAGVPFTVIMFTWSGLACLIFLNCALNWPAEAFPAPEEVDYTKKIKLIGLA
Human LAT3      TFPGIKLIYDAGVAFVVIMFTWSGLACLIFLNCTLNWPIEAFPAPEEVNYTKKIKLSGLA

Mouse LAT3      LDHKVTGDRFYTHVTIVGQRLSQKSPSLEEGADAFISSPDIPGTSEETPEKSVPFRKSLC
Human LAT3      LDHKVTGDLFYTHVTTMGQRLSQKAPSLEDGSDAFMSPQDVRGTSENLPERSVPLRKSLC

Mouse LAT3      SPIFLWSLVTMGMTQLRVIFYMGAMNKILEFIVTGGKERETNEQRQKVEETVEFYSSIFG
Human LAT3      SPTFLWSLLTMGMTQLRIIFYMAAVNKMLEYLVTGGQEHETNEQQQKVAETVGFYSSVFG

Mouse LAT3      VMQLLCLLTCPLIGYIMDWRIKDCVDAPTEGTLNENASFGDARDGASTKFTRPRYRKVQK
Human LAT3      AMQLLCLLTCPLIGYIMDWRIKDCVDAPTQGTV-----LGDARDGVATKSIRPRYCKIQK

Mouse LAT3      LTNAINAFTLTNILLVGFGIACLIKNLHLQLLAFVLHTIVRGFFHSACGGLYAAVFPSNH
Human LAT3      LTNAISAFTLTNLLLVGFGITCLINNLHLQFVTFVLHTIVRGFFHSACGSLYAAVFPSNH

Mouse LAT3      FGTLTGLQSLISAVFALLQQLLFMAMVGPLHGDPFWVNLGLLLLSFLGFLLPSYLYYYRS
Human LAT3      FGTLTGLQSLISAVFALLQQPLFMAMVGPLKGEPFWVNLGLLLFSLLGFLLPSYLFYYRA

Mouse LAT3      RLQREYATNLVDPQKVLNTSKVAT
Human LAT3      RLQQEYAANGMGPLKVLSGSEVTA
```

Figure 1. Alignment of amino acid sequences of mouse and human LAT3 predicted from their nucleotide sequences. The horizontal lines indicate the 12 putative transmembrane domains determined by the TMHMM program (*http://www.cbs.dtu.dk/services/TMHMM/*). The amino acid differences between mouse and human are marked by shading.

Results

Cloning of Mouse LAT3 cDNA

The nucleotide sequencing analysis of mouse LAT3 revealed a single open-reading frame of 2519 nucleotides coding for a predicted protein of 564 amino acids with a deduced molecular weight of 62.6 kd (Figure 1). The deduced amino acid sequence of mouse LAT3 showed 83% identity with that of human LAT3. The ExPASy search showed that mouse LAT3 did not have a signal peptide sequence, even though this molecule contained the motifs for potential *N*- or *O*-glycosylation. Similar to human LAT3,[8] the mouse transporter is predicted to be a 12-transmembrane domain protein and to contain a long intracellular loop between transmembrane domains 6 and 7 with putative protein kinase C-dependent phosphorylation sites (Thr^{231} and Ser^{262}) and a tyrosine phosphorylation site (Thr^{251}).

When expressed in *Xenopus* oocytes, mouse LAT3 induced [^{14}C]L-leucine transport, which was not dependent on Na^+ or Cl^- in the medium (Figure 2, A and B). In addition, substrate selectivity of mouse LAT3 is shown in Figure 2C. Consistent with our previous results of human LAT3,[8] ^{14}C-labeled L-leucine, L-isoleucine, L-valine, and L-phenylalanine were transported at a relatively high rate by mouse LAT3, indicating this molecule distinctly possessed the same functional property as that of human LAT3.

mRNA and Protein Expression of Mouse LAT3

Because our previous study identified the predominant expression of LAT3 transcript in the liver, skeletal muscle, and pancreas in human multiple tissue Northern blots,[8] we first isolated total RNA from these tissues from the fed mice and performed RT-PCR using the specific primer sets for mouse LAT3 and β-actin. As shown in Figure 3, a 572-bp band corresponding to the predicted nucleotide size was detected for the samples from all three tissues

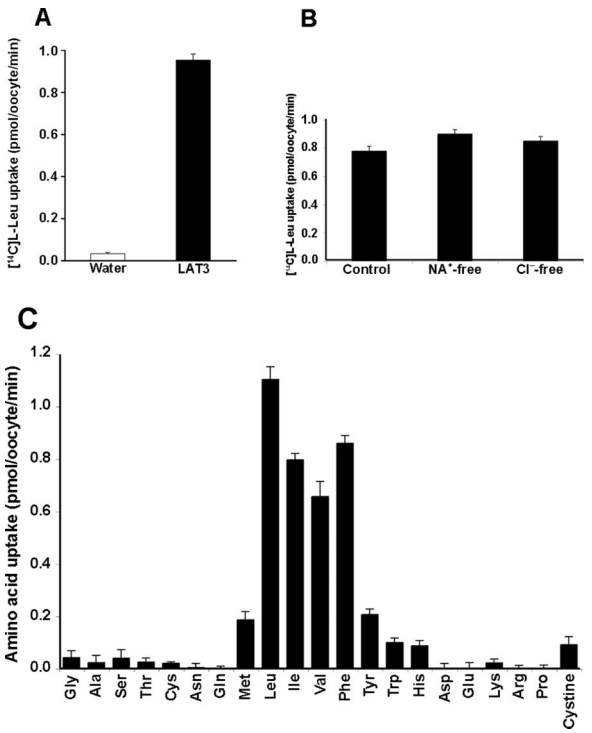

Figure 2. Functional expression of mouse LAT3 in *Xenopus* oocytes. **A:** Uptake of [^{14}C]L-leucine (100 μmol/L) by *Xenopus* oocytes injected with water or LAT3 cRNA (25 ng/oocyte) was measured in Na^+-free uptake solution. **B:** Ion dependence of LAT3-mediated transport. LAT3-mediated [^{14}C]L-leucine uptake (100 μmol/L) measured in the standard uptake solution (Control) was compared with that measured in the Na^+-free uptake solution (Na^+-free) or Cl^--free uptake solution (Cl^--free). **C:** Substrate selectivity of mouse LAT3. LAT3-meditaed ^{14}C-labeled L amino acids were measured in the Na^+-free uptake solution at the concentration of 100 μmol/L.

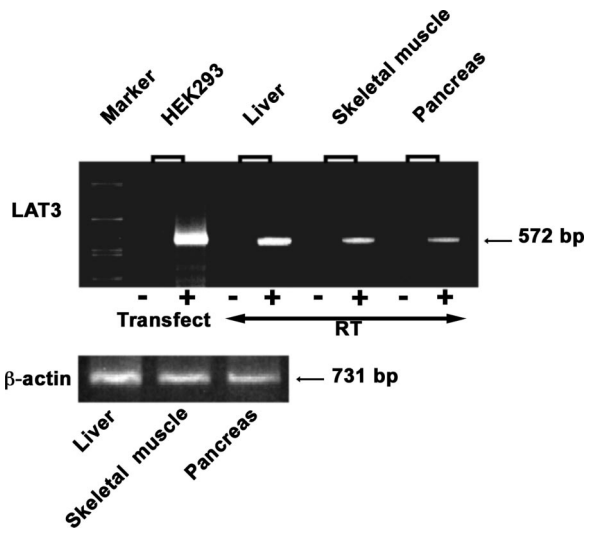

Figure 3. Tissue expression of mouse LAT3 mRNA as detected by RT-PCR. RT-PCR studies were used to amplify mouse β-actin and LAT3-specific sequence. Experiments were performed with reverse transcriptase (RT+) or without RT (RT−) in each step. PCR amplification without RT revealed no PCR product, thereby excluding amplification of genomic DNA. LAT3 mRNA was detected in all three tissues, similarly to how HEK 293 transfected with the mouse LAT3 construct as a positive control.

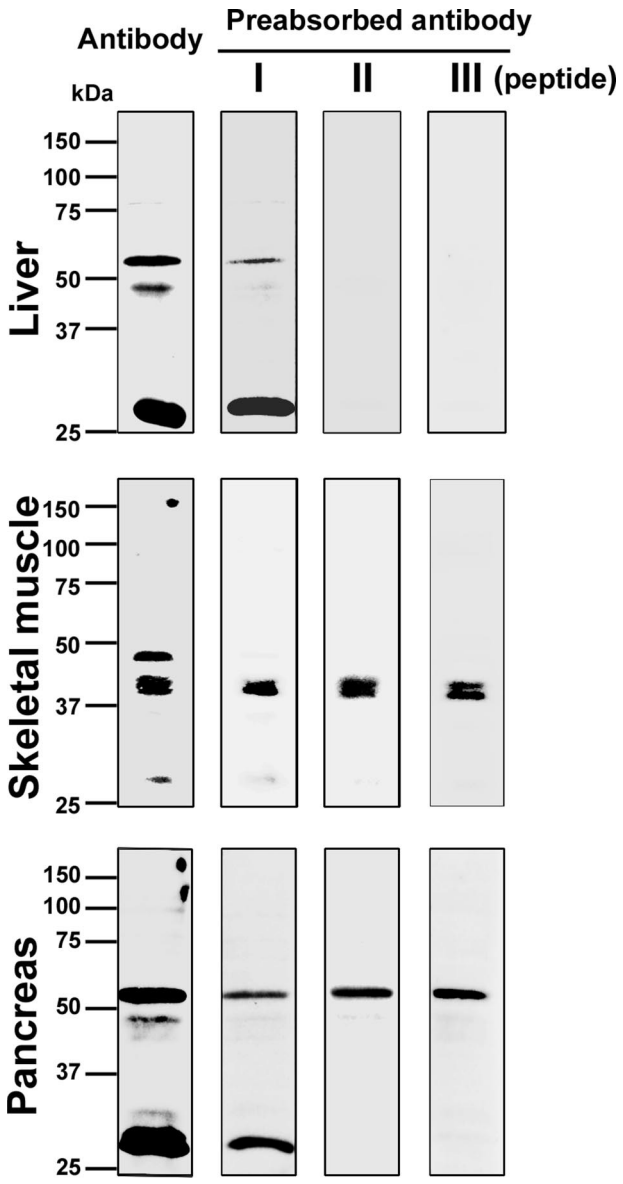

Figure 4. Characterization of the polyclonal antibody against mouse LAT3. Protein samples of the membrane fraction from three tissues (10 μg) were separated on 10% gel and subjected to Western blot analysis with anti-mouse LAT3 polyclonal antibody or anti-mouse LAT3 antibody preabsorbed by the immunogen peptide (peptide II, amino acids 336 to 348) or other synthetic peptides, peptide I (amino acids 336 to 344) and peptide II (amino acids 335 to 349), as described in Materials and Methods. Common specific immunoband in three tissues corresponding to ~48 kd was detected. The protein sample from the liver was also reacted to specific ~58-kd band. Immunoband corresponding to ~28 kd seemed to be degradation of mouse LAT3 in the samples from all three tissues, whereas ~58-kd band in the pancreas sample and ~40-kd band in the skeletal muscle were due to cross-reactivity to an unknown molecule.

as well as for the sample from HEK 293 cells transfected with the mouse LAT3 construct as a positive control. The PCR products were confirmed by direct sequencing to be the mouse LAT3 sequence (data not shown). We next examined the molecular mass of mouse LAT3 protein. To this end, we generated polyclonal antibody against the intracellular domain corresponding to amino acid residues 336 to 348 of mouse LAT3. As depicted in Figure 4, in the liver sample, the antibody reacted with three protein bands that migrated at ~58, ~48, and ~28 kd, respectively. These immunobands tended to partially disappear when the antibody was preabsorbed by peptide I, which was shorter than the immunogen peptide (peptide II; see Materials and Methods). In contrast, preincubation with either peptide II or the longer one (peptide III) completely abolished these positive signals. In the sample from the skeletal muscle, the antibody detected three immunobands that migrated at ~48, ~40, and ~28 kd, and the ~48- and ~28-kd bands completely disappeared by preincubation of the antibody with peptide II or peptide III. However, the ~40-kd band was still visible even when each synthetic peptide was used for the preabsorption, indicating it to be a background signal (Figure 4). Finally, in the sample from the pancreas, again the antibody reacted with three immunobands corresponding to ~58, ~48, and ~28 kd, similar to the liver sample. However, the ~58-kd band was still visible even when the antibody was preabsorbed with peptide III, indicating that this positive signal is a background reaction. In contrast, the ~48- and ~28-kd bands were completely abolished by the preincubation with peptide II or III, suggesting that these two bands are most likely LAT3 in the pancreas (Figure 4).

Cellular and Subcellular Localization of LAT3

We next examined the localization of LAT3 protein in the three organs. In the skeletal muscle, LAT3 was mainly detected in the plasma membrane of the muscle cells (Figure 5A, b and c), and the specificity of this reaction was confirmed by preabsorbing the antibody with the synthetic immunogen peptide, peptide II (Figure 5A, a). On the other hand, we found it to be interesting that the subcellular localization of LAT3 in the pancreas was completely different from that in the muscle cells. At low magnification, LAT3 was strongly detected in the acinar cells (Figure 5B, b) but was not found in the islet cells (data not shown). When viewed at high magnification, a clear reticular pattern was observed in the cytoplasm of the acinar cells (Figure 5B, c). Moreover, interestingly, strong deposits of rod-shaped extensive immunoproduct were detected in the cytoplasm of the acinar cells (Figure 5B, c, arrow). These signals were not seen when antibody preabsorbed with the immunogen peptide was used in place of the anti-mouse LAT3 antibody (Figure 5B, a). In the liver, LAT3 was predominantly localized in the plasma membrane of the hepatocytes and partly in the nucleus and was weakly observed in the cytoplasm (Figure 5C, b–d). The plasma membrane staining of the hepatocytes was clearly visible in both periportal and perivenous regions (Figure 5C, b and c). Moreover, when viewed at high magnification, the distribution of the protein in the plasma membrane of LAT3 was observed basically as a circumferential pattern, including localization in the sinusoidal membrane (Figure 5C, d), whereas no apparent canalicular membrane pattern was seen (Figure 5C, d). No positive signal was seen when immunogen peptide-preabsorbed antibody was used in place of the specific antibody (Figure 5C, a). Because LAT3 of the pancreatic

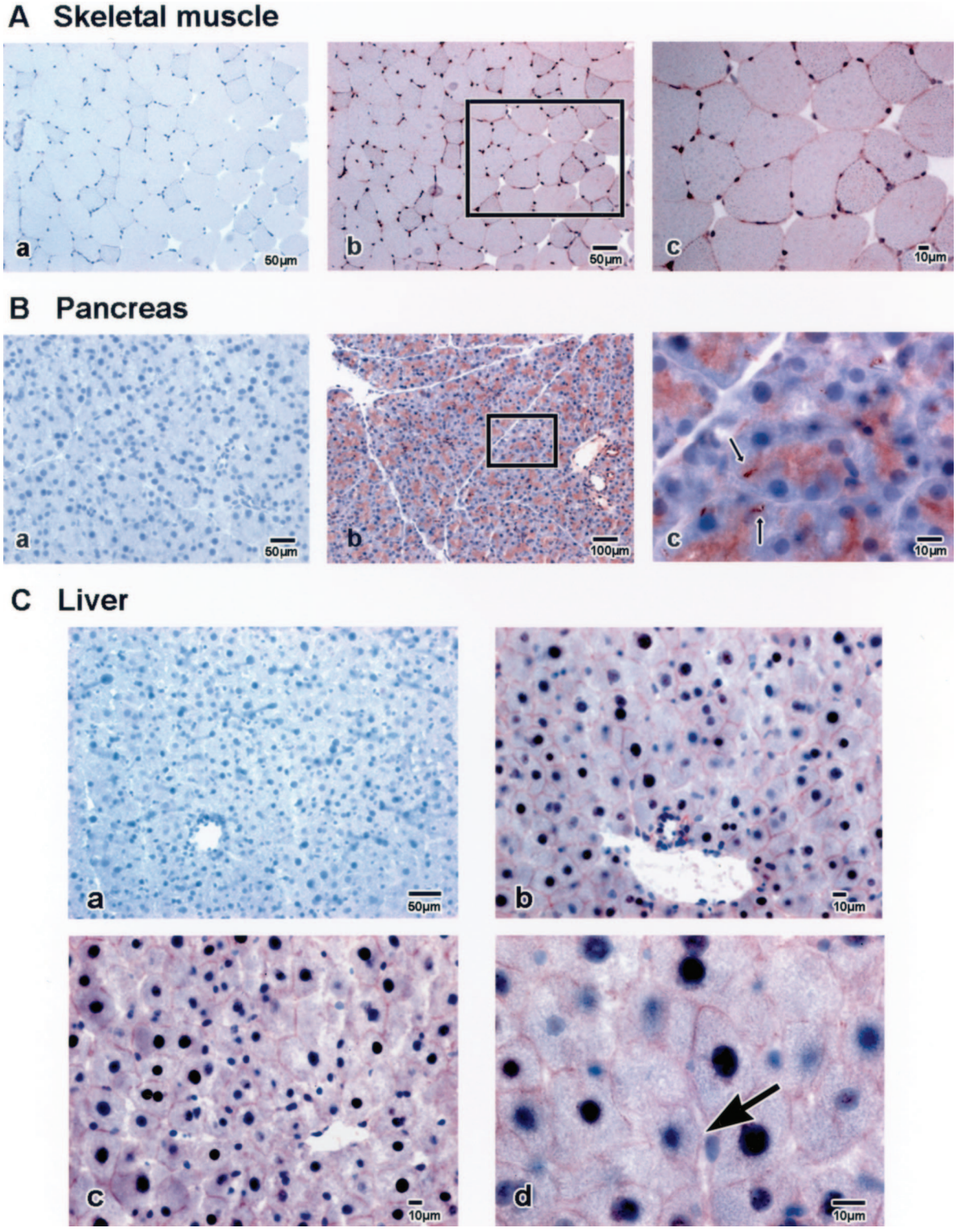

Figure 5. Immunohistochemical analysis of mouse LAT3 in skeletal muscle, pancreas, and liver. **A**, **a:** No immunoproduct is seen in the section reacted with the immunogen peptide-preabsorbed antibody. **b:** Specific antibody detects LAT3 in the plasma membrane of the skeletal muscle. **c:** Enlarged image of rectangle in **b**. **B**, **a:** No positive signal is seen in the section reacted with the immunogen peptide-preabsorbed antibody. **b**, **c:** Specific antibody detects LAT3 in the cytoplasm and the rod-shaped structure of pancreatic acinar cells. **c:** Enlarged image of rectangle in **b**. **C:** LAT3 was predominantly localized in the plasma membrane of the hepatocytes and partly in the nucleus and was weakly observed in the cytoplasm (**b–d**). The plasma membrane staining of the hepatocytes was clearly observed in both periportal (**b**) and perivenous (**c**) region. The protein distribution of LAT3 in the plasma membrane was detected as a circumferential pattern, including the sinusoidal membrane location (**d**, **arrow**), whereas the apparent canalicular membrane pattern was not seen. No positive signal was seen when immunogen peptide-preabsorbed antibody was used in place of the specific antibody (**a**). Sections were counterstained with hematoxylin.

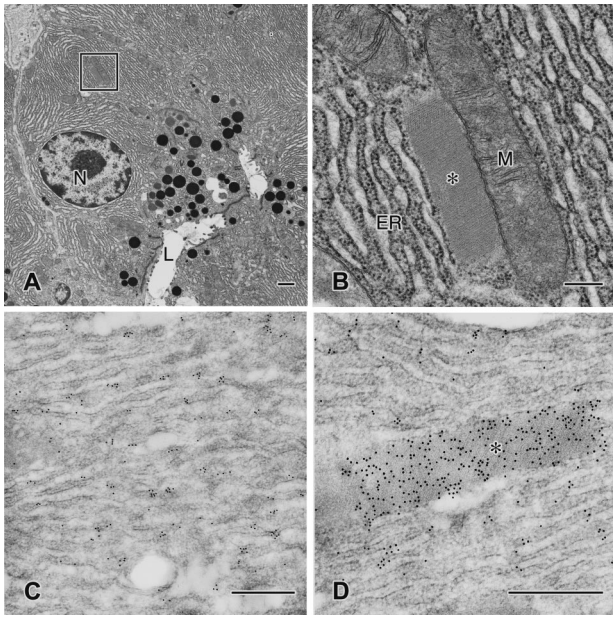

Figure 6. Electron microscopy of LAT3 in mouse pancreas. **A:** Electron micrograph of mouse pancreatic acinar cells observed by conventional electron microscopy. **B:** Enlarged image of rectangle in **A**. Crystal-like structures (**asterisk**) between the endoplasmic reticulum (ER) and the mitochondria (M) can be seen. **C** and **D:** Subcellular localization of LAT3 in pancreatic acinar cells examined by postembedding immunoelectron microscopy. Immunogold particles are densely distributed in the crystal structure as well as in the ER. N, nucleus; L, lumen. Scale bars = 1 μm.

acinar cells was detected in some unknown cytoplasmic structure, we first used conventional electron microscopy to determine its precise structure and then postembedding immunoelectron microscopy to define the exact location of LAT3. Conventional electron microscopy showed the rod-shaped area to be crystalline structures adjacent to the endoplasmic reticulum and the mitochondria in the cytoplasm (Figure 6,A and B). Moreover, the postembedding immunoelectron microscopy determined LAT3 to be located in these crystalline structures as well as in the endoplasmic reticulum (Figure 6, C and D).

Effect of Nutrient Starvation on LAT3 Expression

We used immunofluorescence and confocal microscopy to determine whether any difference in the expression level or distribution pattern of mouse LAT3 could be induced by nutrient starvation. Before this experiment, to confirm that energy deprivation distinctly occurs in the mice starved for 24 hours, we examined sections of the liver obtained from fed mice and starved ones by conventional electron microscopy. As depicted in Figure 7A, the glycogen granules in the hepatocytes of the starved mice were drastically decreased in number compared with those of the fed mice. In addition, the mitochondria tended to have contracted to various degrees and displayed disrupted cristae, suggesting the actual existence of a nutrient deficiency in their body. Under this starvation condition, although there was no drastic change seen in the distribution pattern of LAT3 in the liver, the immunofluorescence intensity of this transporter in the plasma membrane as well as in the cytoplasm was apparently increased compared with that in the control (fed) mice (Figure 7B). In addition, the immunofluorescence intensity of LAT3 in the plasma membrane of skeletal muscle cells was also increased by the nutrient starvation (Figure 7B). Finally, in the pancreas, nutrient starvation resulted in an increased number of the rod-shaped LAT3-positive structures in the acinar cells but did not induce its appearance in the plasma membrane of these cells (Figure 7B).

Next, we conducted RT-PCR and Western blot analysis using these tissues from fed and starved mice to compare the expression of LAT3 semiquantitatively at both transcript and protein levels. As depicted in Figure 7C, nutrient starvation apparently stimulated the mRNA expression of LAT3 in both the liver and the skeletal muscle but not in the pancreas. Moreover, the starvation accelerated the production of LAT3 protein in the liver, as evidenced by the apparent increase in the density of the ~58- and ~48-kd bands (Figure 7D). Nutrient starvation also increased the amount of LAT3 protein (~48 kd) in the skeletal muscle (Figure 7D); however, there was no obvious change in the protein level of the ~48-kd form of LAT3 in the starved pancreas (Figure 7D). Finally, we examined RT-PCR with LAT1 and LAT2 using liver and skeletal muscle to determine whether this increase of LAT3 is specific for energy starvation. As illustrated in Figure 7E, there was no drastic change like LAT3 of both mRNA in starved liver and skeletal muscle compared with fed one; only a slightly upward trend of LAT1 in starved liver was visible.

Discussion

To date, four system L amino acid transporters, including the recently cloned LAT4,[19] have been identified at the molecular level; however, little is yet known about their protein character and functional property *in vivo*. The first identified isoform was LAT1, the transcripts of which are widely expressed in many nonepithelial cells such as those in the lung, spleen, thymus, brain, placenta, skin, liver, and testis, as well as in activated peripheral leukocytes.[20] However, despite its well-known expression in many malignant cells,[21,22] in normal tissues, the protein has been shown to be distributed only in the plasma membrane of vascular endothelial cells forming the blood-brain barrier[23,24] and of syncytiotrophoblastic cells in the placenta.[25] The second protein identified, LAT2, is highly expressed in polarized cells such as those in the small intestine and proximal tubules of the kidney,[4–6,26] suggesting its crucial role in transepithelial amino acid transport. Although the amino acid specificity and apparent affinity are different between LAT1 and LAT2,[20] both transporters require the heavy chain of the 4F2 antigen to express their functional property on the plasma membrane.

We recently cloned a third Na^+-independent system L neutral amino acid transporter, LAT3, from a human hepatocarcinoma cell line.[8] To specify the protein characteristics of this molecule, and because its transcript was identified to be prominently expressed in the liver,

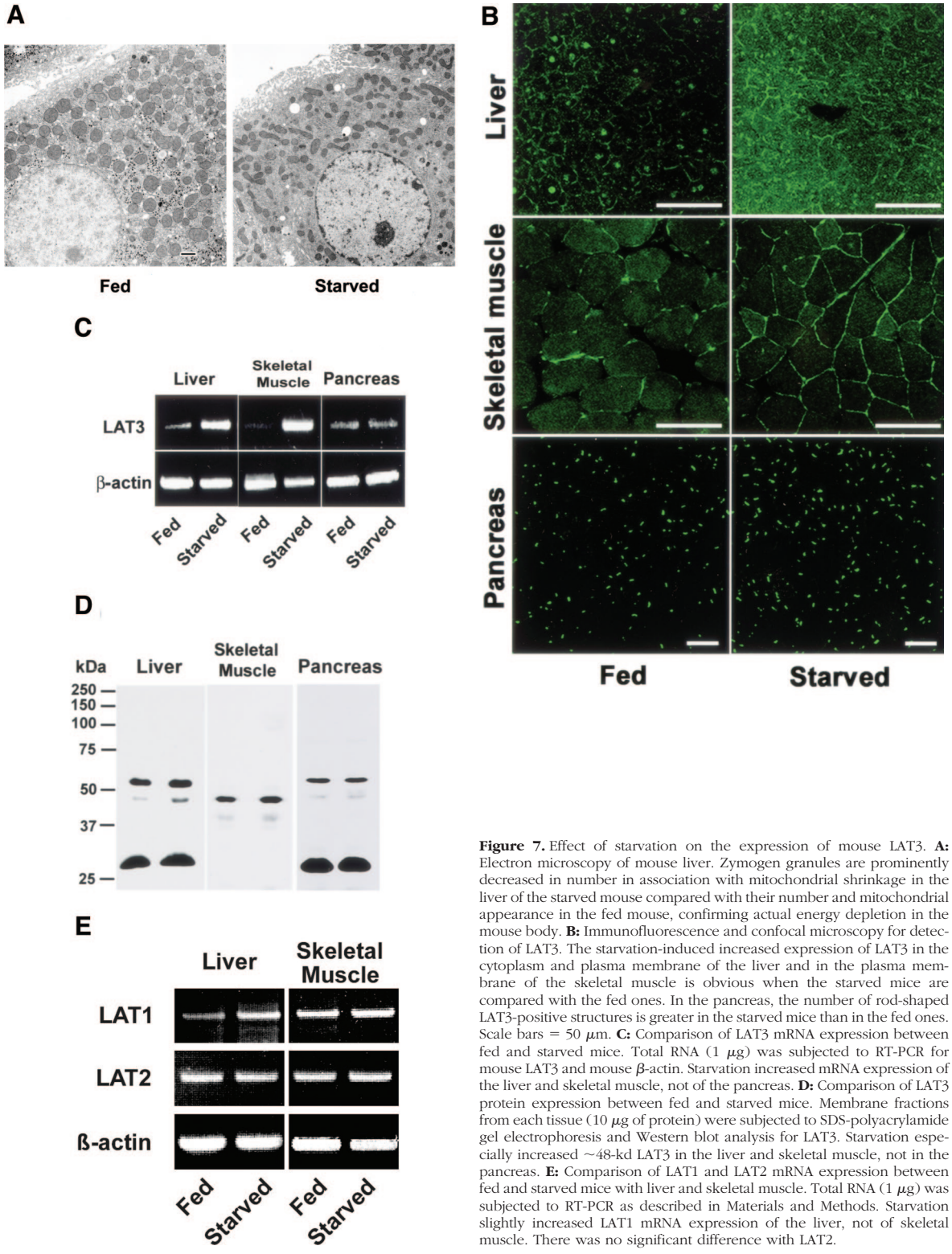

Figure 7. Effect of starvation on the expression of mouse LAT3. **A:** Electron microscopy of mouse liver. Zymogen granules are prominently decreased in number in association with mitochondrial shrinkage in the liver of the starved mouse compared with their number and mitochondrial appearance in the fed mouse, confirming actual energy depletion in the mouse body. **B:** Immunofluorescence and confocal microscopy for detection of LAT3. The starvation-induced increased expression of LAT3 in the cytoplasm and plasma membrane of the liver and in the plasma membrane of the skeletal muscle is obvious when the starved mice are compared with the fed ones. In the pancreas, the number of rod-shaped LAT3-positive structures is greater in the starved mice than in the fed ones. Scale bars = 50 μm. **C:** Comparison of LAT3 mRNA expression between fed and starved mice. Total RNA (1 μg) was subjected to RT-PCR for mouse LAT3 and mouse β-actin. Starvation increased mRNA expression of the liver and skeletal muscle, not of the pancreas. **D:** Comparison of LAT3 protein expression between fed and starved mice. Membrane fractions from each tissue (10 μg of protein) were subjected to SDS-polyacrylamide gel electrophoresis and Western blot analysis for LAT3. Starvation especially increased ~48-kd LAT3 in the liver and skeletal muscle, not in the pancreas. **E:** Comparison of LAT1 and LAT2 mRNA expression between fed and starved mice with liver and skeletal muscle. Total RNA (1 μg) was subjected to RT-PCR as described in Materials and Methods. Starvation slightly increased LAT1 mRNA expression of the liver, not of skeletal muscle. There was no significant difference with LAT2.

skeletal muscle, and pancreas by using human multiple tissue Northern blots, in the present study, we focused on the identification of the protein expression and the distribution of its homologue in the same organs in mice. To this end, we first cloned mouse LAT3 cDNA and showed it to have 83% identity with human LAT3. The expression experiments using *Xenopus* oocytes clearly demonstrated that the mouse LAT3 predominantly transported neutral amino acids such as L-leucine, L-isoleucine, L-valine, and L-phenylalanine in a Na^+-independent manner, indicating that mouse LAT3 possessed the same functional property as human LAT3.

For immunohistochemistry, we generated specific antibody by immunizing a rabbit with synthetic peptide corresponding to amino acids 336 to 348 of mouse LAT3. To assess the specificity of this antibody, we conducted a preabsorption experiment with Western blot analysis by using not only the immunogen peptide but also a shorter peptide and the longer peptide compared with the immunogen peptide (see Materials and Methods). Overall, although the strong ~28-kd band observed in all three tissues was completely abolished by the predasorption with the immunogen peptide or the longer one, this molecular weight seems to be too small compared with the deduced molecular weight of 62.6 kd; thus, this band most likely reflects a degradation product of LAT3. The antibody also detected a ~48-kd immunoband, which was found for all three tissues. Although it may still seem small compared with the deduced molecular mass, this immunoband possibly reflects the proper mouse LAT3. Indeed, it was earlier shown that the molecular mass of mouse LAT2 is ~42 kd despite its deduced molecular mass of 57.9 kd.[5] Moreover, human LAT1 is also understood to be a ~38-kd protein despite its deduced molecular mass of 55.1 kd.[22] The reason for this discrepancy between the relative migration on SDS gels and the deduced molecular weight in the LAT family needs to be further investigated. Finally, a ~58-kd band was also seen in the samples from both the liver and pancreas but not in those from the skeletal muscle. However, it is not likely that these ~58-kd bands are the same isoform in these two tissues because in the liver this immunoband was completely abolished by preabsorption of the antibody with the immunogen peptide or the longer one, whereas that of the pancreas was not lost. Two-dimensional electrophoresis followed by Western blot analysis with LAT3 may solve this inconsistent result. Taken together, our data indicate that, excluding the degradation product, the liver expresses two isoforms of LAT3, ie, ~58- and ~48-kd ones, and that both the skeletal muscle and pancreas express only the ~48-kd form.

Using this specific antibody, the subcellular localization of LAT3 in three tissues from the fed mice was investigated. The results with the liver and skeletal muscle seemed to be reasonable because the plasma membrane localization in both tissues was apparent. However, in pancreatic acinar cells, an unexpected localization pattern of LAT3 was observed by light microscopy, in which the pattern of rod-shaped structures predominated. To determine the nature of these structures, we performed electron microscopy on the pancreas of fed mice. Interestingly, specific crystalline-like structures were found in the cytoplasm of the acinar cells. These structures were most likely the so-called crystalline inclusions reported to exist in many organs and many species.[27] Although the acinar cells of the rodent pancreas were also apparently shown to possess these structures,[28,29] their molecular nature has not yet been elucidated. Our result showing the increased number of LAT3-positive structures in the pancreatic acinar cells of the starved mice suggests that this molecule may respond to the alteration in the energy balance. However, based on its nature of being found in crystal structures not bound by the plasma membrane, the positive signal of LAT3 in this structure is most likely an artifact due to cross-reactivity. In addition, although the immunoelectron microscopy clearly detected LAT3 signals in the pancreatic endoplasmic reticulum (ER), starvation did not increase the expression level of mRNA and protein there, indicating that LAT3 in the pancreas is not likely to be involved in the overall response of the mouse body to starvation.

We previously showed that a single injection of mouse LAT3 cRNA was sufficient for the functional expression of this isoform in *Xenopus* oocytes,[8] indicating that LAT3 does not require the N-glycoprotein 4F2hc to assemble to the plasma membrane, unlike LAT1 and LAT2. Recently, another new system L transporter, LAT4, has been identified by homology to LAT3.[19] This isoform is an *N*-glycosylated protein which was cleaved by glycosidase treatment, suggesting no involvement of 4F2hc in expressing its functional property on the plasma membrane. In contrast, although our ExPASy search showed that LAT3 contained the motifs for potential *N*- or *O*-glycosylation on its amino acid sequence, it seems not to be a glycoprotein because we could not find any shifted migration of LAT3 when the protein lysates from any of the tissues were treated with *N*-glycosidase F and *O*-glycosidase (data not shown). Therefore, we speculate that some other type of post-translational modification may be involved in the plasma membrane assembly of LAT3 in the liver and skeletal muscle.

Substrate selectivity of LAT3 is distinct from that of LAT1 and LAT2.[8] LAT3 shows narrower substrate selectivity than LAT1 and LAT2 and mainly transports BCAAs and phenylalanine. BCAAs (leucine, isoleucine, and valine) are essential amino acids that serve as essential substrates in the synthesis of proteins and represent the major nitrogen source for glutamine and alanine synthesis in the muscle. The importance of BCAAs as metabolic fuel during the stressful situations of caloric deprivation (starvation) and increased caloric need (exercise) has been concluded from recent observations.[30–32] Under a stressful situation, the first step in BCAA catabolism is reversible transamination leading to the production of the corresponding branched-chain keto acids (BCKAs), which occurs mainly in skeletal muscle, a tissue having high BCAA aminotransferase activity.[33] Then BCKAs are released into the bloodstream and taken up by different tissues where they can be oxidized or used for the resynthesis of BCAAs. Several studies have shown that synthesis of BCAAs from BCKAs is favorable in hepatic tissue[34,35]; therefore, it is suggested that there is a cycle of BCAA and BCKA transport between the muscle and liver.[36] In the present study, we determined that starvation increased the protein expression of LAT3 in the hepatic cells and muscle cells. Based on the functional property of LAT3, in which transport of BCAAs is electroneutral and mediated by facilitated diffusion,[8] we speculate the mechanism underlying the functional role of LAT3 in the liver and skeletal muscle to be as follows: first, starvation causes an energy-deficient status in the body, where glycogen is immediately used for glucose production in the liver as a compensatory response. This

was clearly confirmed by the drastic decrease in the content of glycogen granules in the hepatic cells, as was observed by electron microscopy. Together with this, an increase in proteolysis in skeletal muscle occurs, resulting in the accelerated catabolism of BCAAs to BCKAs, which is accompanied by glutamine and alanine synthesis. Then, in the liver, alanine is used as an important precursor for gluconeogenesis. Concurrently, BCKAs excreted from the skeletal muscle is taken up in the liver, where BCAAs are re-synthesized from BCKAs more than in the fed situation. This increased production of BCAAs in the liver might induce up-regulation of LAT3 to excrete BCAAs into the bloodstream via facilitated diffusion. Indeed, it is known that the concentration of BCAAs in the blood is increased during starvation in humans[37–40] and rats.[41,42] In addition, in the isolated perfusion-liver model, starvation accelerates the excretion of BCAAs from the liver into the bloodstream.[42] Moreover, when the amino acid concentrations are compared between the portal vein and hepatic vein during starvation, most amino acids flow from the extrahepatic tissue to liver, whereas BCAAs flow in the opposite direction.[43] In addition, it is well known that BCAAs are also released by the skeletal muscle itself and that their level is increased twofold by starvation.[40,44] These facts and the up-regulation of LAT3 protein in the plasma membrane observed in the present study suggest that LAT3 may directly transport BCAAs from the cytoplasm of the hepatic cells and muscle cells into the bloodstream under the starvation condition, resulting in the essential supply of BCAAs to other energy-depleted organs such as the brain. It is important to know whether the increase of LAT3 in liver and skeletal muscle is specific for energy deprivation. We noticed that only LAT1 mRNA from starved liver was shown to slightly increase compared with that from fed liver. However, whether LAT1 protein could indeed exist and function in liver remains unclear. Because the size of the LAT1 transcript was revealed to be shorter than the other tissues like brain and placenta, the further protein work should be examined to solve its real function under energy starvation condition.[45] Finally, the meaning of the existence of LAT3 in the pancreas is still unknown. Our result revealed that LAT3 of the pancreas might not function at least after birth even under starved situation. Because several amino acid transporters such as SNAT1[46] and ASC1[47] have been identified at the protein level, the potential role of these molecules in the pancreas under the nutrient-starved condition should be further studied.

Acknowledgments

We are grateful to Dr. Hitoshi Takenaka for helpful discussion and comments on this work before publication. We also thank S. Matsubara for excellent technical assistance.

References

1. Christensen HN: Role of amino acid transport and countertransport in nutrition and metabolism. Physiol Rev 1990, 70:43–77
2. Palacín M, Estevez R, Bertran J, Zorzano A: Molecular biology of mammalian plasma membrane amino acid transporters. Physiol Rev 1998, 78:969–1054
3. Kanai Y, Segawa H, Miyamoto K, Uchino H, Takeda E, Endou H: Expression cloning and characterization of a transporter for large neutral amino acids activated by the heavy chain of 4F2 antigen (CD98). J Biol Chem 1998, 273:23629–23632
4. Pineda M, Fernandez E, Torrents D, Estevez R, Lopez C, Camps M, Lloberas J, Zorzano A, Palacin M: Identification of a membrane protein, LAT2, that co-expresses with 4F2 heavy chain, an L-type amino acid transport activity with broad specificity for small and large zwitterionic amino acids. J Biol Chem 1999, 274:19738–19744
5. Rossier G, Meier C, Bauch C, Summa V, Sordat B, Verrey F, Kuhn LC: LAT2, a new basolateral 4F2hc/CD98-associated amino acid transporter of kidney and intestine. J Biol Chem 1999, 274:34948–34954
6. Segawa H, Fukasawa Y, Miyamoto K, Takeda E, Endou H, Kanai Y: Identification and functional characterization of a Na^+-independent neutral amino acid transporter with broad substrate selectivity. J Biol Chem 1999, 274:19745–19751
7. Verrey F: System L: heteromeric exchangers of large, neutral amino acids involved in directional transport. Pflugers Arch 2003, 445: 529–533
8. Babu E, Kanai Y, Chairoungdua A, Kim do K, Iribe Y, Tangtrongsup S, Jutabha P, Li Y, Ahmed N, Sakamoto S, Anzai N, Nagamori S, Endou H: Identification of a novel system L amino acid transporter structurally distinct from heterodimeric amino acid transporters. J Biol Chem 2003, 278:43838–43845
9. Martinet W, De Meyer GR, Andries L, Herman AG, Kockx MM: In situ detection of starvation-induced autophagy. J Histochem Cytochem 2006, 54:85–96
10. Mizushima N, Yamamoto A, Matsui M, Yoshimori T, Ohsumi Y: In vivo analysis of autophagy in response to nutrient starvation using transgenic mice expressing a fluorescent autophagosome marker. Mol Biol Cell 2004, 15:1101–1111
11. Kanai Y, Nussberger S, Romero MF, Boron WF, Hebert SC, Hediger MA: Electrogenic properties of the epithelial and neuronal high affinity glutamate transporter. J Biol Chem 1995, 270:16561–16568
12. Utsunomiya-Tate N, Endou H, Kanai Y: Cloning and functional characterization of a system ASC-like Na^+-dependent neutral amino acid transporter. J Biol Chem 1996, 271:14883–14890
13. Fujii Y, Khoshnoodi J, Takenaka H, Hosoyamada M, Nakajo A, Bessho F, Kudo A, Takahashi S, Arimura Y, Yamada A, Nagasawa T, Ruotsalainen V, Tryggvason K, Lee AS, Yan K: The effect of dexamethasone on defective nephrin transport caused by ER stress: a potential mechanism for the therapeutic action glucocorticoids in the acquired glomerular diseases. Kidney Int 2006, 69:1350–1359
14. Nishibori Y, Liu L, Hosoyamada M, Endou H, Kudo A, Takenaka H, Higashihara E, Bessho F, Takahashi S, Kershaw D, Ruotsalainen V, Tryggvason K, Khoshnoodi J, Yan K: Disease-causing missense mutations in NPHS2 gene alter normal nephrin trafficking to the plasma membrane. Kidney Int 2004, 66:1755–1765
15. Yan K, Kudo A, Hirano H, Watanabe T, Tasaka T, Kataoka S, Nakajima N, Nishibori Y, Shibata T, Kohsaka T, Higashihara E, Tanaka H, Watanabe H, Nagasawa T, Awa S: Subcellular localization of glucocorticoid receptor protein in the human kidney glomerulus. Kidney Int 1999, 56:65–73
16. Akimoto Y, Yamamoto K, Munemoto E, Wells L, Vosseller K, Hart GW, Kawakami H, Hirano H: Elevated post-translational modification of proteins by O-linked N-acetylglucosamine in various tissues of diabetic Goto-Kakizaki rats accompanied by diabetic complications. Acta Histochem Cytochem 2005, 38:131–142
17. Akimoto Y, Kreppel LK, Hirano H, Hart GW: Localization of the O-linked N-acetylglucosamine transferase in rat pancreas. Diabetes 1999, 48:2407–2413
18. Ohara-Imaizumi M, Ohtsuka T, Matsushima S, Akimoto Y, Nishiwaki C, Nakamichi Y, Kikuta T, Nagai S, Kawakami H, Watanabe T, Nagamatsu S: ELKS, a protein structurally related to the active zone-associated protein CAST, is expressed in pancreatic beta cells and functions in insulin exocytosis: interaction of ELKS with exocytotic machinery analyzed by total internal reflection fluorescence microscopy. Mol Biol Cell 2005, 16:3289–3300
19. Bodoy S, Martin L, Zorzano A, Palacin M, Estevez R, Bertran J: Identification of LAT4, a novel amino acid transporter with system L activity. J Biol Chem 2005, 280:12002–12011

20. Wagner CA, Lang F, Broer S: Function and structure of heterodimeric amino acid transporters. Am J Physiol Cell Physiol 2001, 281:C1077–C1093
21. Nakanishi K, Matsuo H, Kanai Y, Endou H, Hiroi S, Tominaga S, Mukai M, Ikeda E, Ozeki Y, Aida S, Kawai T: LAT1 expression in normal lung and in atypical adenomatous hyperplasia and adenocarcinoma of the lung. Virchows Arch 2005, 21:1–9
22. Yanagida O, Kanai Y, Chairoungdua A, Kim DK, Segawa H, Nii T, Cha SH, Matsuo H, Fukushima J, Fukasawa Y, Tani Y, Taketani Y, Uchino H, Kim JY, Inatomi J, Okayasu I, Miyamoto K, Takeda E, Goya T, Endou H: Human L-type amino acid transporter 1 (LAT1): characterization of function and expression in tumor cell lines. Biochim Biophys Acta 2001, 1514:291–302
23. Matsuo H, Tsukada S, Nakata T, Chairoungdua A, Kim DK, Cha SH, Inatomi J, Yorifuji H, Fukuda J, Endou H, Kanai Y: Expression of a system L neutral amino acid transporter at the blood-brain barrier. Neuroreport 2000, 11:3507–3511
24. Boado RJ, Li JY, Nagaya M, Zhang C, Pardridge WM: Selective expression of the large neutral amino acid transporter at the blood-brain barrier. Proc Natl Acad Sci USA 1999, 96:12079–12084
25. Ritchie JW, Taylor PM: Role of the system L permease LAT1 in amino acid and iodothyronine transport in placenta. Biochem J 2001, 356:719–725
26. Dave MH, Schulz N, Zecevic M, Wagner CA, Verrey F: Expression of heteromeric amino acid transporters along the murine intestine. J Physiol 2004, 558:597–610
27. Ghadially FN: Ultrastructural Pathology of the Cell and Matrix. Edited by FN Ghadially. Newton, Butterworth-Heinemann, 1997, pp 1038–1045
28. Papadimitriou JM, Walters MN, Archer JM: Cytoplasmic crystalline aggregates in murine pancreatic acinocytes. Pathology 1969, 1:289–293
29. Machino M, Hoshino K: Membrane unbound crystals in pancreatic acinar cells of the mouse. Virchows Arch B Cell Pathol 1975, 17:261–267
30. Adibi SA, Krzysik BA, Morse EL, Amin PM, Allen ER: Oxidative energy metabolism in the skeletal muscle: biochemical and ultrastructural evidence for adaptive changes. J Lab Clin Med 1974, 83:548–562
31. Goldberg AL, Odessey R: Oxidation of amino acids by diaphragms from fed and fasted rats. Am J Physiol 1972, 223:1384–1391
32. Ahlborg G, Felig P, Hagenfeldt L, Hendler R, Wahren J: Substrate turnover during prolonged exercise in man: splanchnic and leg metabolism of glucose, free fatty acids, and amino acids. J Clin Invest 1974, 53:1080–1090
33. Harper AE, Miller RH, Block KP: Branched-chain amino acid metabolism. Annu Rev Nutr 1984, 4:409–454
34. Livesey G, Lund P: Enzymic determination of branched-chain amino acids and 2-oxoacids in rat tissues: transfer of 2-oxoacids from skeletal muscle to liver in vivo. Biochem J 1980, 188:705–713
35. Abumrad NN, Robinson RP, Gooch BR, Lacy WW: The effect of leucine infusion on substrate flux across the human forearm. J Surg Res 1982, 32:453–463
36. Holecek M: Relation between glutamine, branched-chain amino acids, and protein metabolism. Nutrition 2002, 18:130–133
37. Adibi SA, Drash AL: Hormone and amino acid levels in altered nutritional states. J Lab Clin Med 1970, 76:722–732
38. Adibi SA: Influence of dietary deprivations on plasma concentration of free amino acids of man. J Appl Physiol 1968, 25:52–57
39. Felig P, Owen OE, Wahren J, Cahill Jr GF: Amino acid metabolism during prolonged starvation. J Clin Invest 1969, 48:584–594
40. Swendseid ME, Umezawa CY, Drenick E: Plasma amino acid levels in obese subjects before, during, and after starvation. Am J Clin Nutr 1969, 22:740–743
41. Ahlman B, Andersson K, Leijonmarck CE, Ljungqvist O, Hedenborg L, Wernerman J: Short-term starvation alters the free amino acid content of the human intestinal mucosa. Clin Sci (Lond) 1994, 86:653–662
42. Holecek M, Sprongl L, Tilser I: Metabolism of branched-chain amino acids in starved rats: the role of hepatic tissue. Physiol Res 2001, 50:25–33
43. Bloxam DL: Nutritional aspects of amino acid metabolism. Br J Nutr 1972, 27:233–247
44. Pozefsky T, Tancredi RG, Moxley RT, Dupre J, Tobin JD: Effects of brief starvation on muscle amino acid metabolism in nonobese man. J Clin Invest 1976, 57:444–449
45. Prasad PD, Wang H, Huang W, Kekuda R, Rajan DP, Leibach FH, Ganapathy V: Human LAT1, a subunit of system L amino acid transporter: molecular cloning and transport function. Biochem Biophys Res Commun 1999, 255:283–288
46. Weiss MD, Donnelly WH, Rossignol C, Varoqui H, Erickson JD, Anderson KJ: Ontogeny of the neutral amino acid transporter SNAT1 in the developing rat. J Mol Histol 2005, 36:301–309
47. Hashimoto Y, Sadamoto Y, Konno A, Kon Y, Iwanaga T: Distribution of neutral amino acid transporter ASCT1 in the non-neuronal tissues of mice. Jpn J Vet Res 2004, 52:113–122